ELECTROMAGNETIC RADIATION FROM PRINTED TRACES ON A CIRCUIT BOARD WITH COATED PLASTIC COVER

Jean-Fu Kiang

IBM T. J. Watson Research Center
Yorktown Heights, NY 10598

Abstract

A rigorous formulation in the spectral domain is used to investigate the radiation from printed traces on a circuit board in the frequency range from 30 MHz to 1 GHz. Both the coupling effect among adjacent traces and the shielding effectiveness of metallic coating on the plastic cover are analyzed. It is found that the radiation around resonant frequencies is critical to satisfy the FCC requirement, and an appropriate coating can resolve the problem.

INTRODUCTION

The radiation characteristics of microstrip antennas have been widely studied mainly for applications in communications[1], [2]. However, they are scarcely considered in the printed circuit boards used in the frequency range from 30 MHz to 1 GHz. The understanding of radiation properties in this frequency range is necessary to have the circuit boards satisfy the FCC requirements.

A metallic coating on the plastic cover has been used to shield radiation from terminals to the neighboring equipment. However, little information is available about its effectiveness. In [3], the shielding effectiveness of a metallic coating is studied. A plane wave of normal incidence is assumed, and the shielding effectiveness is a function of the material properties only. In [4], the radiating sources of high impedance and low impedance nature are also considered. However, the results can not be used to study the radiation from printed traces on a circuit board since the radiating sources of the latter are more complicated.

In this paper, we apply a spectral domain formulation to printed traces radiating in a stratified medium. The substrate, plastic cover, and the metallic coating are all considered as layers of the stratified medium. The surface currents on the printed traces are represented by a set of rooftop basis functions[5]. The Galerkin's method[6] is used to solve the integral equation for the current distribution. The radiation field can be obtained by stationary phase integration method[7]. The effects of geometrical parameters and material properties are also investigated.

MATHEMATICAL FORMULATION

The geometrical configuration of parallel traces on a circuit board with cover is shown in Figure 1, where there are S parallel traces embedded in layer (m) of a general stratified medium consisting of $(n+1)$ layers. The stratification is perpendicular to the z axis, the conductivity, dielectric constant, and thickness of layer (m) are σ_m, ε_m, and h_m, respectively. All the traces are assumed to lie along the y direction, the width and length of the sth trace are w_s and L_s, respectively.

The field expressions in layer (l) can be represented by the dyadic Green's function and the surface current in layer (m) as [6], [7]

$$\bar{E}(\bar{r}) = i\omega\mu_0 \int\int dS' \bar{\bar{G}}_{lm}(\bar{r}, \bar{r}') \cdot \bar{J}_s(\bar{r}') \tag{1}$$

where $\bar{J}_s(\bar{r}')$ is the surface current on the printed traces. The dyadic Green's function $\bar{\bar{G}}_{lm}(\bar{r}, \bar{r}')$ can be represented in the spectral domain as

$$\bar{\bar{G}}_{lm}(\bar{r}, \bar{r}') = \frac{i}{8\pi^2} \int\int_{-\infty}^{\infty} d\bar{k}_s e^{i\bar{k}_s \cdot (\bar{r}_s - \bar{r}'_s)} \bar{\bar{g}}_{lm}(\bar{k}_s, z, z') \tag{2}$$

where $\bar{\bar{g}}_{lm}(\bar{k}_s, z, z')$ is the Fourier transform of $\bar{\bar{G}}_{lm}(\bar{r}, \bar{r}')$.

For $l < m$, the explicit form of $\bar{\bar{g}}_{lm}(\bar{k}_s, z, z')$ is given by

$$\begin{aligned}
\bar{\bar{g}}_{lm}(\bar{k}_s, z_>, z'_<) = {} & \frac{X^{\mathrm{TE}}_{\cup l}}{k_{mz}(1 - R^{\mathrm{TE}}_{\cup m} R^{\mathrm{TE}}_{\cap m} e^{2ik_{mz}h_m})} \\
& \left[\hat{h}(k_{lz}) e^{ik_{lz}z_l} + R^{\mathrm{TE}}_{\cup l} \hat{h}(-k_{lz}) e^{ik_{lz}(2h_l - z_l)}\right] \\
& \left[\hat{h}(k_{mz}) e^{-ik_{mz}z'_m} + R^{\mathrm{TE}}_{\cap m} \hat{h}(-k_{mz}) e^{ik_{mz}(2h_m + z'_m)}\right] \\
& + \frac{X^{\mathrm{TM}}_{\cup l}}{k_{mz}(1 - R^{\mathrm{TM}}_{\cup m} R^{\mathrm{TM}}_{\cap m} e^{2ik_{mz}h_m})} \\
& \left[\hat{v}(k_{lz}) e^{ik_{lz}z_l} + R^{\mathrm{TM}}_{\cup l} \hat{v}(-k_{lz}) e^{ik_{lz}(2h_l - z_l)}\right] \\
& \left[\hat{v}(k_{mz}) e^{-ik_{mz}z'_m} + R^{\mathrm{TM}}_{\cap m} \hat{v}(-k_{mz}) e^{ik_{mz}(2h_m + z'_m)}\right]
\end{aligned} \tag{3}$$

where z_l and z'_m are the local coordinates defined as $z_l = z + d_l$, $z'_m = z' + d_{m-1}$; $\hat{h}(\pm k_{bz})$ and $\hat{v}(\pm k_{bz})$ are the polarization vectors in layer b with $b = l, m$; $X^a_{\cup l}$ is the upward transmission

CH2848-0/90/0000-0697$01.00 © 1990 IEEE

coefficient of mode α with α = TE or TM, respectively; R^{α}_{ul} (R^{α}_{nl}) is the upward (downward) reflection coefficient at the upper (lower) boundary of layer (l). Both the transmission and reflection coefficients can be calculated recursively. For $l = m$ and $l > m$, similar expressions as (3) can be obtained.

The field expressions in (1)-(3) satisfy all the boundary conditions at the interfaces between adjacent layers. We impose the remaining boundary condition that the total tangential electric field vanishes on the surfaces of the printed traces, assuming that the traces are made of perfect conductor. Thus, we obtain the following coupled integral equations :

$$\bar{E}_{m\perp}(\bar{r}) - \bar{E}^{i}_{\perp}(\bar{r}) = 0, \qquad \bar{r} \text{ on } A_k, \qquad 1 \le k \le S \tag{4}$$

where $\bar{E}_{m\perp}(\bar{r})$ is the tangential electric field in layer (m) generated by the surface current on the traces, A_k is the surface of the kth trace, $\bar{E}^{i}_{\perp}(\bar{r})$ is the tangential electric field generated by the excitation sources, which are assumed to be delta gaps in this paper.

NUMERICAL SOLUTION

On general circuit boards, the length of a trace is much longer than the width; hence, the transversal surface current is much smaller than the longitudinal one , and can be neglected. To solve (4), we first choose a set of rooftop basis functions to represent the surface current as

$$\bar{J}_s(\bar{r}_s) = \hat{y} \sum_{j=1}^{N_s} \alpha_{sj} Q(x - x_{sj}, w_s) P(y - y_{sj}, l_s) \tag{5}$$

where $1 \le s \le S$, $\alpha_{sj}{}'$ s are the unknowns to be solved, (x_{sj}, y_{sj}) is the center coordinate of the jth basis function on the sth trace, N_s is the number of basis functions on the sth trace, and $l_s = 2L_s/(N_s + 1)$. $Q(x - x_{sj}, w_s)$ and $P(y - y_{sj}, l_s)$ are pulse and triangle functions, respectively.

Next, substituting (5) into (1), and imposing the boundary condition in (4), we obtain a set of coupled integral equations. The Galerkin's method[6] is then applied to solve the integral equations for the current distribution. The stationary phase integration method[7] is used to obtain the far field pattern.

RESULTS AND DISCUSSIONS

In Fig. 2(a), we present the magnitude of current moment on a printed trace as a function of frequency. The current moment on trace k is defined as

$$\bar{m}_k = \int\int_{A_k} dxdy \bar{J}_s(\bar{r}_s) \tag{6}$$

where $\bar{J}_s(\bar{r}_s)$ is the current distribution on trace k. In general, the magnitude increases with frequency. Around the resonant frequency, the magnitude increases by more than two orders.

The input resistance and reactance of the same trace are shown in Figs. 2(b) and 2(c), respectively. It is found that the input resistance is negligibly small below the resonant frequency, and possesses a peak around 940 MHz. The magnitude of input reactance is much larger than that of input resistance below the resonant frequency, and reduces to zero around the resonant frequency. The input reactance switches from a large negative number to a large positive number around 940 MHz, which is typical of a thin antenna.

This implies that the printed trace behaves like a capacitor at low frequency with little radiation, and like an antenna around resonant frequency.

The radiation field patterns on the E-plane (YZ-plane) and the H-plane (XZ -plane) are shown in Fig. 2(d). It is observed that at low frequencies, the radiation is tolerable to the FCC requirement, but around the resonant frequency, the radiation is far above the requirement.

Next, we study the coupling effect between two identical traces parallel to each other. In Fig. 3, the magnitude of current moment for both the common and the differential modes are displayed as a function of frequency.

The resonant frequency of the common mode is different from that of the differential mode. In general, the radiation from a common mode is much stronger than that from a differential mode, especially in the low frequency range. However, the situation is reversed near the resonant frequency of the differential mode.

In Fig. 4, we present the field pattern calculated at a distance of three meters at f = 850 MHz. The metallic coating is made of copper. As the coating thickness increases, the magnitude of E_{ϕ} on the H-plane decreases, and the patterns are roughly the same. The magnitude of E_{θ} on the E-plane reduces significantly around the z direction as the coating thickness is increased. However, the reduction is not so obvious as the zenith angle is increased. This can be explained as follows : the current on the trace induces electric current inside the metallic coating. The field generated by the induced current cancells a significant portion of the field generated by the trace in the broadside directions, but the cancellation is less effective around the axial direction of the trace.

To summarize the usefulness of metallic coating, we define the shielding effectiveness ($S.E.$) as

$$S.E. = 20 \log_{10} \left| \frac{E_{t,\max}(\text{without shield})}{E_{t,\max}(\text{with shield})} \right|. \tag{7}$$

The shielding effectiveness in [3] is defined as the ratio of field magnitude at the same location before and after the shield is inserted. Since the plane wave of normal incidence is assumed, there is no need to consider the location of maximum field strength. However, in this problem, the field pattern changes before and after the shield is inserted; and the FCC requirement is imposed on the maximum field strength in any possible direction. Hence, it is appropriate to use the definition in (7).

In Fig. 5, we present the shielding effectiveness of metallic coatings with three different thicknesses and two different conductivities. It is observed that the shielding effectiveness increases with increasing frequency, conductivity, or physical thickness.

CONCLUSIONS

A rigorous formulation in the spectral domain is used to investigate the radiation characteristics of printed traces in the presence of adjacent traces and coated cover. The resonant frequencies for different trace configurations and driving source arrangements are studied, and have to be considered in the design phase of a circuit board. The shielding effectiveness is also analyzed. Appropriate use of metallic coating can effectively shield the radiation.

Acknowledgment

The author wishes to thank D. J. McBride, B. J. Rubin, and S. Daijavad for their useful comments and discussions.

References

[1] I. J. Bahl and P. Bhartia, *Microstrip Antennas* , Dedham, MA : Artech House, 1980.

[2] K. R. Carver and J. W. Mink, "Microstrip antenna technology," *IEEE Trans.* AP-29, no. 1, pp.2-24, January 1981.

[3] S. Y. Liao, "RF shielding effectiveness and light transmission of copper or silver film coating on plastic substrate," *IEEE Trans.* EMC-18, no. 4, pp.148-153, November 1976.

[4] R. B. Schulz, V. C. Plantz, and D. R. Brush, "Shielding theory and practice," *IEEE Trans.* EMC-30, no. 3, pp.187-201, August, 1988.

[5] B. J. Rubin, "The propagation characteristics of signal lines in a mesh-plane environment," *IEEE Trans.* MTT-32, no. 5, pp.522-531, May 1984.

[6] J. F. Kiang, S. M. Ali, and J. A. Kong, "Propagation properties of striplines periodically loaded with crossing strips," *IEEE Trans.* MTT-37, no. 4, pp.776-786, April 1989.

[7] J. A. Kong, *Electromagnetic Waves Theory* , New York : Wiley, 1986.

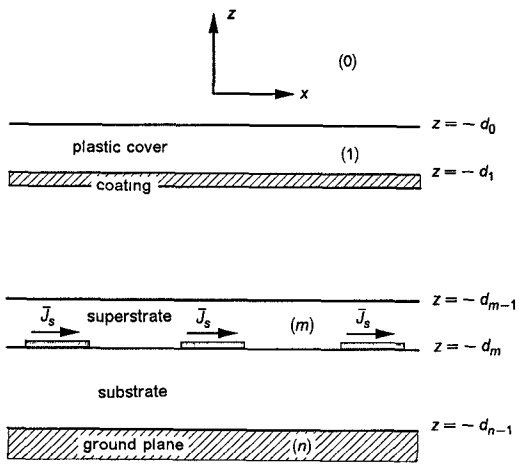

Fig. 1 : Geometrical configuration of printed traces embedded in a multi-layered medium.

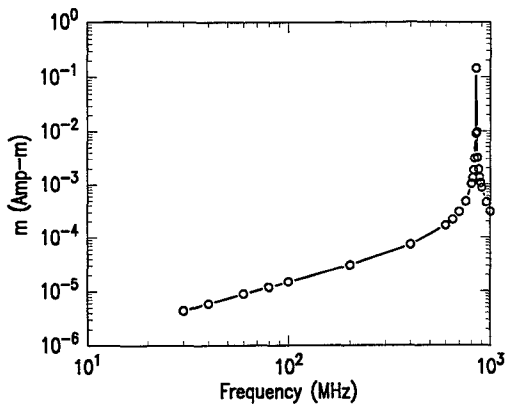

Fig. 2(a) : Magnitude of current moment on a printed trace, $l_1 = 10$ cm, $w_1 = 150\mu$ m, a delta gap of 1 volt is located 1 cm from one end, $\varepsilon_{r0} = 1.0$, $\varepsilon_{r1} = 4.7$, $\varepsilon_{r2} = 1.0$, $\sigma_0 = 0$, $\sigma_1 = 0$, $\sigma_2 = 5.92 \times 10^7$ S/m, $h_1 = 500\mu$ m.

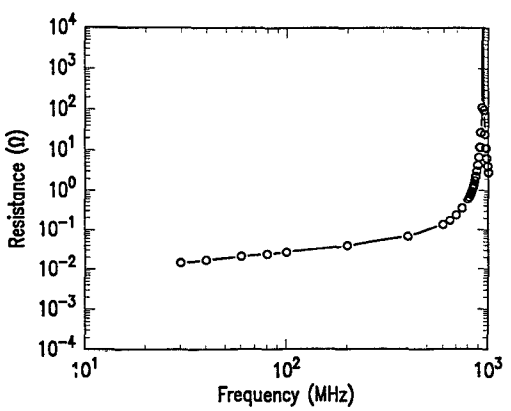

Fig. 2(b) : Input resistance he same printed trace as in Fig. 2(a).

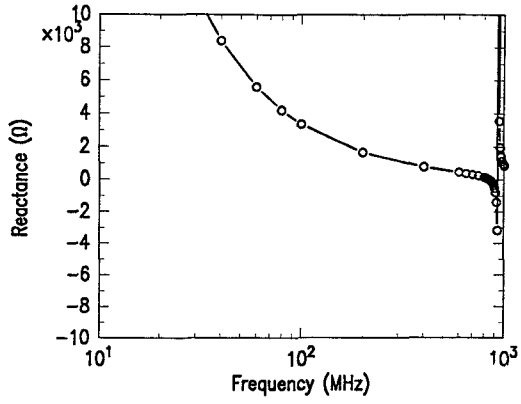

Fig. 2(c) : Input reactance of the same printed trace as in Fig. 2(a).

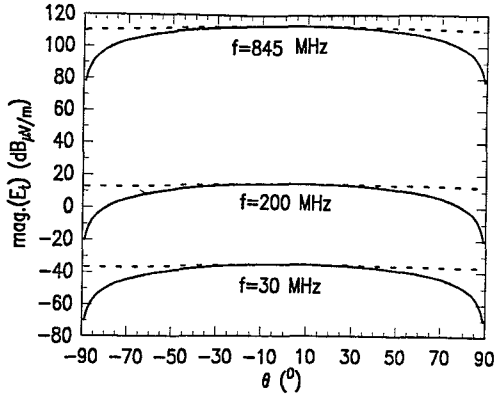

Fig. 2(d) : Magnitude of tangential electric field calculated at 3 m from the same printed trace as in Fig. 2(a),——— E_ϕ at $\phi = 0°$,– – – – E_θ at $\phi = 90°$.

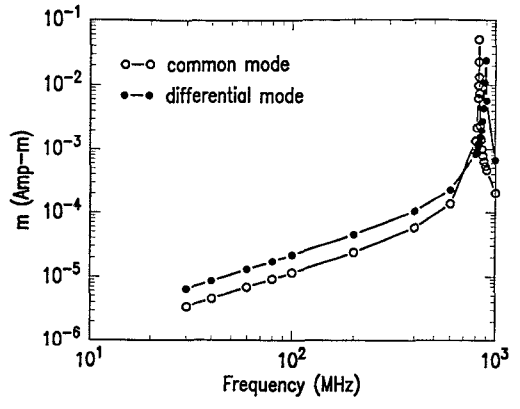

Fig. 3 : Magnitude of current moment on two printed traces, $l_1 = l_2 = 10$ cm, $w_1 = w_2 = 150\mu$m, center-to-center separation is 300 μm, $\varepsilon_{r0} = 1.0$, $\varepsilon_{r1} = 4.7$, $\varepsilon_{r2} = 1.0$, $\sigma_0 = 0$, $\sigma_1 = 0$, $\sigma_2 = 5.92 \times 10^7$ S/m, $h_1 = 500\mu$m, delta gaps of 1 volt are located 1 cm from one end of each trace.

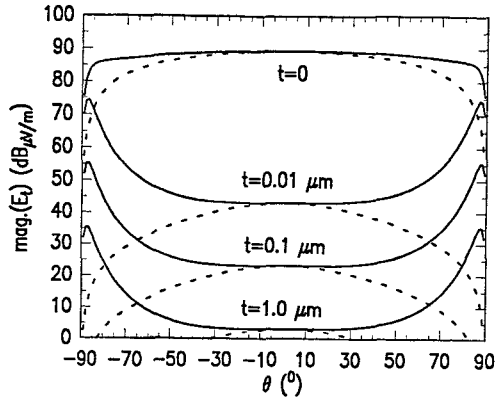

Fig. 4 : Magnitude of tangential electric field calculated at 3 m, f=850 MHz, $l_1 = 10$ cm, $w_1 = 150\mu$m, a delta gap of 1 volt is located 1 cm from one end, $\varepsilon_{r0} = 1.0$, $\varepsilon_{r1} = 2.7$, $\varepsilon_{r2} = 1.0$, $\varepsilon_{r3} = 1.0$, $\varepsilon_{r4} = 4.7$, $\varepsilon_{r5} = 1.0$, $\sigma_0 = 0$, $\sigma_1 = 0$, $\sigma_2 = \sigma_5 = 5.92 \times 10^7$ S/m, $\sigma_3 = 0$, $\sigma_4 = 0$, $h_1 = 0.5$ cm, $h_2 = t$, $h_3 = 10$ cm, $h_4 = 500\mu$ m,– – – – E_ϕ at $\phi = 0°$,——— E_θ at $\phi = 90°$.

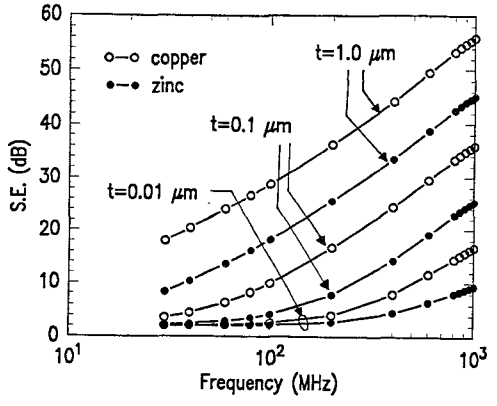

Fig. 5 : Shielding effectiveness of metallic coating on radiation from a printed trace with the same parameters as in Fig. 4.